The Bell System Technical Journal
Vol. 52, No. 6, July–August, 1973
Printed in U.S.A.

Impulse Response of Clad Optical Multimode Fibers

By D. GLOGE

(Manuscript received January 9, 1973)

Loss, coupling, and delay differences among the modes of multimode fibers influence their response to intensity-modulated optical signals. This "baseband" response is derived here from a time-dependent continuous description of the power flow in the fiber. Particular attention is given to the output as a function of angle and to the impulse response, its width and symmetry. We find that coupling narrows the impulse response but, at the same time, causes additional loss. Under practical conditions, this loss may limit the usefulness of coupling for the purpose of reducing the mode dispersion. We calculate a possible data rate of 12 Mb/s for a 10-km repeater spacing and an effective numerical aperture of 0.1, but we show that further improvements can be gained from an optimization of the coupling characteristic and of other parameters.

I. INTRODUCTION

Although single-mode operation of clad optical fibers is possible and, in general, offers very good transmission characteristics, multimode fibers have two advantages: They impose less stringent requirements on the optical carrier (they transmit even the incoherent light from a luminescent diode) and their larger dimensions alleviate splicing problems or at least relax the tolerances required for connection. Typically, the core diameter is of the order of a hundred wavelengths and the fiber therefore transmits thousands of modes, even if the index difference between core and cladding is only a few percent (corresponding to a numerical aperture of 0.2 to 0.3).

The usefulness of such fibers depends on their dispersion characteristics. Delay differences among the many modes[1] distort the signal and certainly produce a signal response inferior to that of the single-mode fiber. For certain systems, on the other hand, overall system economy may place the desirable information rate of individual fiber channels

in a range where the characteristic signal response of multimode fibers is adequate (below 100 megabits per second, say). In such systems, multimode operation would surpass single-mode operation because of the advantages mentioned earlier.

Effective use of the multimode fiber would presuppose the excitation of a large number of modes right at the input with the objective of transmitting *all* of these modes to the receiver. Experiments that have approximated these conditions have revealed a rather intricate response to short input pulses both in liquid- and solid-core multimode fibers.[2,3] For example, the width of the output pulse did not increase linearly with fiber length, but showed a less-than-proportional increase for long fibers. Coupling among the modes and a dependence of loss on mode number seemed to play a part.[4] In some fibers, this resulted in an optimal mode distribution (causing lowest overall loss) which comprised only a fraction of the modes capable of propagating. Measurements of the coupling strength showed that a total exchange of power between two modes was likely to occur within less than a meter of fiber.[5] This result made it clear that a perturbation theory depending on small coupling rates was not applicable. A closed and unrestricted description was achieved by assuming a modal continuum rather than thousands of individual modes. In this theory, mode coupling took the form of a diffusion process not limited to small coupling amplitudes.

The work discussed here extends the approach outlined in Ref. 5 by taking the velocity differences among the modes into account. We first consider fibers in which the optimal (steady-state) mode distribution does not include modes close to cutoff. The power in the fiber is calculated as a function of time and output angle (mode number) for the case of a short input pulse. Particular attention is given to the "fiber impulse response" obtained by integrating over all angles at the output. A simple formula relates the output pulse width to the fiber length and to the attenuation and coupling parameters. The latter can be measured in short samples (a few meters in length) permitting the immediate computation of the pulse broadening in a long fiber and, hence, of the obtainable data rate for a given fiber length.

The results may also shed some light on the prospects of mode coupling introduced artificially as a means of equalization: It has been predicted that, under certain circumstances, increased mode coupling reduces the signal distortion (ultimately forcing all energy to propagate at an average velocity).[6,7] The objective of this paper is to outline an analytic approach which can answer these and other questions.

II. TIME-DEPENDENT POWER FLOW EQUATION

The differential equation obtained in Ref. 5 for the power flow in multimode fibers was originally derived from the mode characteristics by assuming certain statistics for the modal field coupling. By making some approximations acceptable for high-order modes, a description results which admits a simple ray-optics interpretation. Each high-order mode can be represented by a characteristic ray propagating inside the core along a meridional zigzag path. Internal reflection guides the rays at the core-cladding interface and limits the range of angles which can be formed with the guide axis. If n and n_c are the indices of core and cladding, respectively, and

$$\Delta = 1 - \frac{n_c}{n} \tag{1}$$

is a small difference, the maximum angle is given by the condition of critical internal reflection which is approximately

$$\theta_{\max} = \sqrt{2\Delta}. \tag{2}$$

The rays form a uniform distribution within the cone of apex angle $\theta_{\max}$.

If the core cross section permits many modes to propagate, the rays are so densely spaced that their distribution can be considered as continuous. The state of the fiber at a point z and at time t can then be described by a distribution $P(\theta, z, t)$ where θ is a continuous variable.* Reference 5 expresses the incremental change dP in the power P as a sum of two terms:

(*i*) A loss $-A\theta^2 P dz$; this term comprises attenuation effects in the cladding and the core-cladding interface and increases as the square of the characteristic angle θ. The coefficient A is measured in $\mathrm{m}^{-1}\,\mathrm{rad}^{-2}$. θ-independent loss is omitted, but can easily be incorporated later in the final solution.

(*ii*) Mode coupling; in practical multimode fibers, coupling was found to occur essentially only between closely adjacent modes and, for this reason, takes the form of a diffusion process in the ray picture. The incremental increase in $P(\theta, z)$ as a result of diffusion is $(1/\theta)(\partial/\partial\theta)(\theta D \partial P/\partial\theta)dz$, a term typical for radial diffusion in cylindrical configurations. D is a coupling coefficient

* θ is related to the transverse wave number u of the corresponding mode by $u = nk\theta$ where k is the vacuum wave number.

which, for most of the following discussion, is assumed to be independent of θ.

The total variation in P thus becomes

$$dP = -A\theta^2 P dz + \frac{1}{\theta}\frac{\partial}{\partial\theta}\left(\theta D \frac{\partial P}{\partial\theta}\right) dz. \tag{3}$$

If P is a function of time t, we can also write

$$dP = \frac{\partial P}{\partial z} dz + \frac{\partial P}{\partial t} dt. \tag{4}$$

Equating (3) and (4) and dividing by dz results in the equation

$$\frac{\partial P}{\partial z} + \frac{dt}{dz}\frac{\partial P}{\partial t} = -A\theta^2 P + \frac{1}{\theta}\frac{\partial}{\partial\theta}\left(\theta D \frac{\partial P}{\partial\theta}\right). \tag{5}$$

The derivative dz/dt is the velocity of the power $P(\theta)$ or, equivalently, the group velocity of a mode with characteristic angle θ. By using the relation between θ and the transverse wave number u, we can calculate this velocity from eq. (25) of Ref. 8. Except for the few modes close to cutoff, we obtain the simple relation

$$\frac{dz}{dt} = \frac{c}{n(1 + \theta^2/2)}. \tag{6}$$

It relates the mode velocity to the vacuum light velocity, c, reduced by n because of the material retardation and by a factor $1 + \theta^2/2$ which accounts for the increased path length as a result of the zigzag propagation. The derivative dt/dz required in (5) is the inverse of (6) and has the meaning of a delay per unit length. If we ignore the delay n/c common to all modes (it can be added later if necessary), we obtain from (5) and (6)

$$\frac{\partial P}{\partial z} = -A\theta^2 P - \frac{n}{2c}\theta^2 \frac{\partial P}{\partial t} + \frac{1}{\theta}\frac{\partial}{\partial\theta}\left(\theta D \frac{\partial P}{\partial\theta}\right). \tag{7}$$

With the help of the Laplace transformation

$$p(\theta, z, s) = \int_0^\infty e^{-st} P(\theta, z, t) dt, \tag{8}$$

we can write (7) in the form

$$\frac{\partial p}{\partial z} = -A\sigma^2\theta^2 p + \frac{1}{\theta}\frac{\partial}{\partial\theta}\left(\theta D \frac{\partial p}{\partial\theta}\right) \tag{9}$$

where

$$\sigma = (1 + ns/2cA)^{\frac{1}{2}}. \tag{10}$$

Except for the factor σ^2, (9) agrees with (22) of Ref. 5; we can therefore use the solution derived there if we replace A by $A\sigma^2$. For the Gaussian input distribution

$$p_{in} = f(0, s) \exp(-\theta^2/\Theta_o^2), \tag{11}$$

we obtain

$$p(\theta, z, s) = f(z, s) \exp[-\theta^2/\Theta^2(z, s)] \tag{12}$$

where

$$\Theta^2(z, s) = \frac{\Theta_\infty^2}{\sigma} \frac{\sigma\Theta_o^2 + \Theta_\infty^2 \tanh \sigma\gamma_\infty z}{\Theta_\infty^2 + \sigma\Theta_o^2 \tanh \sigma\gamma_\infty z} \tag{13}$$

and

$$f(z, s) = \frac{f(0, s)\sigma\Theta_o^2}{\Theta_\infty^2 \sinh \sigma\gamma_\infty z + \sigma\Theta_o^2 \cosh \sigma\gamma_\infty z} \tag{14}$$

with

$$\Theta_\infty = (4D/A)^{\frac{1}{2}} \tag{15}$$

and

$$\gamma_\infty = (4DA)^{\frac{1}{2}}. \tag{16}$$

For cw excitation ($s = 0$), the angular width $\Theta(z, 0)$ changes monotonically from Θ_o to Θ_∞ as z increases. The width Θ_∞ characterizes a distribution which propagates unchanged (at steady state) and with the minimum overall loss coefficient γ_∞. It seems practical to excite this distribution right from the beginning. The condition $\Theta_o = \Theta_\infty$ will therefore receive particular attention in the following. The solutions (12) through (16) assume that Θ_o and Θ_∞ are so small compared to $\theta_{max} = \sqrt{2\Delta}$ that practically no light propagates at angles close to the critical one. In other words, modes close to cutoff do not take part in the transmission process. Experiments have shown that the steady state in certain liquid-core fibers ($C_2C\ell_4$ in quartz, for example) is of that type.

Closed-form Laplace transformations of (12) exist only for the approximations given in the limits $z \ll 1/\gamma_\infty$ and $z \gg 1/\gamma_\infty$ and these two cases are discussed in Section III. Certain important characteristics of $P(\theta, z, t)$, however, can be derived for all z, as we shall see in Section IV.

III. CLOSED-FORM SOLUTIONS FOR THE IMPULSE RESPONSE

In a practical communication system, the multimode fiber is likely to be fed with a pulse $F(0, t)$ whose width is typically of the same order as the broadening expected in the fiber. Its Laplace transform $f(0, s)$, appearing in (12) and (14), and its dependence on s therefore cannot be ignored. We assume, however, that the input is simultaneous in all modes being excited, in which case Θ_o is independent of s. Sacrificing

generality for clarity, we restrict this discussion to the practical input condition $\Theta_o = \Theta_\infty$; the general case can be treated in exactly the same way, but leads to more complicated results.

In the case of a short fiber, we replace $\sinh \sigma\gamma_\infty z$ and $\tanh \sigma\gamma_\infty z$ in (13) and (14) by the argument $\sigma\gamma_\infty z$ and set $\cosh \sigma\gamma_\infty z = 1$. With the help of (10), (15), and (16), (12) then becomes

$$p(\theta, z, s) = \frac{f(0, s)}{1 + \gamma_\infty z} \exp\left[-\theta^2\left(\frac{1}{\Theta_o^2} + \frac{nz}{2c}s\right)\right] \tag{17}$$

which has the Laplace transform

$$P(\theta, z, t) = \frac{\exp(-\theta^2/\Theta_o^2)}{1 + \gamma_\infty z} F(0, t - n\theta^2 z/2c). \tag{18}$$

The denominator $1 + \gamma_\infty z$ expresses the loss in the short distance z; $\exp(-\theta^2/\Theta_o^2)$ indicates that the input condition has been conserved, and $F(0, t - n\theta^2 z/2c)$ shows that the portion of the input pulse $F(0, t)$ which propagated at an angle θ was delayed by $n\theta^2 z/2c$. Clearly, coupling has not affected the propagation at this distance.

The total output is obtained from the integration[5]

$$q(z, s) = 2\pi \int_0^\infty p(\theta, z, s)\theta d\theta. \tag{19}$$

For $z \ll 1/\gamma_\infty$, we obtain with (17)

$$q = \frac{\pi f(0, s)\Theta_o^2}{(1 + \gamma_\infty z)(1 + n\Theta_o^2 zs/2c)}. \tag{20}$$

If we now set $f(0, s) = 1$, which corresponds to an infinitesimally short input pulse of energy 1, the Laplace transformation of (20) yields the impulse response of the fiber:

$$Q(z, t) = \frac{2c\pi}{nz(1 + \gamma_\infty z)} \exp(-2ct/n\Theta_o^2 z). \tag{21}$$

The assumption of a mode continuum has the consequence that the impulse response is a continuous and well-behaved function, in spite of the somewhat artificial condition of an infinitesimally narrow input pulse. That Q extends mathematically to infinity results from the assumption of the unbounded distributions (11) and (12). Remember that this assumption was acceptable since $\Theta_o = \Theta_\infty < \theta_{\max}$. The same condition limits $Q(t)$ practically to a time interval narrower than $n\theta_{\max}^2 z/2c$, which is the delay between the fastest and the slowest mode. Since (18) and (21) neglect mode coupling, they could have been ob-

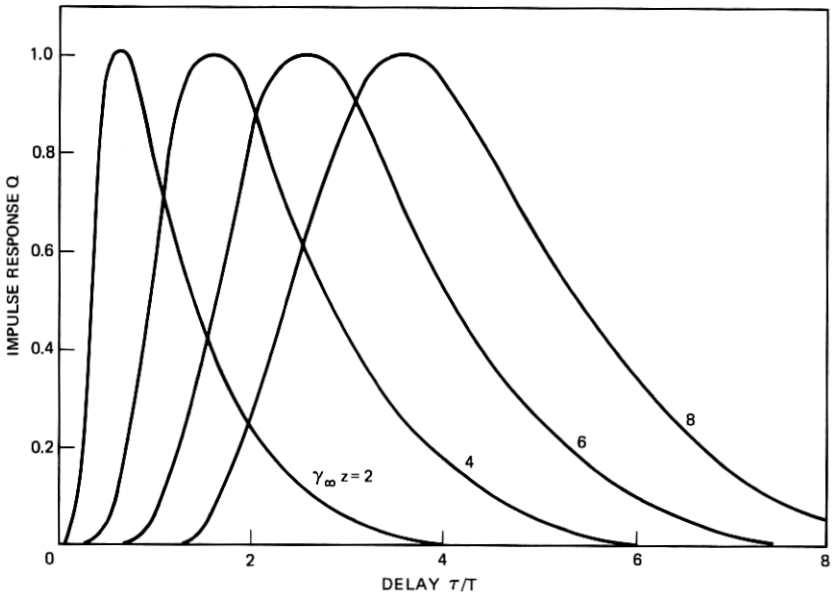

Fig. 1—Impulse response according to (24) normalized for equal peak values and plotted versus normalized time for different fiber lengths.

tained without the help of the power flow equation. They were derived here merely for a better understanding of the physical implications involved.

In the case of a very long fiber, we may use the approximation $\tanh \sigma\gamma_\infty z = 1$ and $\sinh \sigma\gamma_\infty z = \cosh \sigma\gamma_\infty z = \frac{1}{2} \exp \sigma\gamma_\infty z$ in (13) and (14). Equation (12) thus assumes the form

$$p = \frac{2\sigma}{1+\sigma} \exp\left[-\sigma(\theta^2/\Theta_o^2 + \gamma_\infty z)\right] \tag{22}$$

which leads to

$$q = \frac{2\pi\Theta_o^2}{1+\sigma} \exp\left(-\sigma\gamma_\infty z\right) \tag{23}$$

where p is integrated over all angles θ with the help of (19). After introducing (10) for σ into (23) we can form the Laplace transform of $q(s)$. By using the condition $\gamma_\infty z > 1$, we arrive at

$$Q(z, t) = \Theta_o^2 \sqrt{\frac{\pi}{Tt}} \left(\frac{t}{\gamma_\infty z T} + \frac{1}{2}\right)^{-1} \exp\left(-\frac{\gamma_\infty^2 z^2 T}{4t} - \frac{t}{T}\right) \tag{24}$$

where

$$T = \frac{n}{2cA} = \frac{n}{2c} \frac{\Theta_o^2}{\gamma_\infty}. \tag{25}$$

An evaluation of (24) is shown in Fig. 1 for various normalized lengths $\gamma_\infty z$. The plotted impulse responses are normalized for equal peak values.

The normalizing distance $1/\gamma_\infty$ is the distance within which a 1-neper loss is incurred as a result of the θ-dependent loss characteristic. Note that additional θ-independent loss can be present. As indicated by (21), T is the $1/e$-width, which the impulse response Q would assume at the distance $1/\gamma_\infty$ if no coupling were present. Closed-form solutions for Q are available only in the two cases discussed here, but another very practical characterization of the fiber output distribution can be obtained without performing the Laplace transformation.

IV. PULSE DELAY AND PULSE WIDTH

Because of a general relation between $P(t)$ and its Laplace transform $p(s)$, we obtain the mth moment of $P(t)$ from

$$(-1)^m \frac{\partial^m p}{\partial s^m}\bigg|_{s=0} = \int_0^\infty t^m P dt. \tag{26}$$

To achieve a suitable normalization we set $m = 0$ which yields

$$p(s = 0) = \int_0^\infty P dt \tag{27}$$

and divide (26) through (27). This leads to

$$(-1)^m \frac{\partial^m \ell n p}{\partial s^m}\bigg|_{s=0} = \frac{\int_0^\infty (t - \delta)^m P dt}{\int_0^\infty P dt}, \tag{28}$$

where

$$\delta = \frac{\int_0^\infty (-t) P dt}{\int_0^\infty P dt} = -\frac{\partial \ell n p}{\partial s}\bigg|_{s=0}. \tag{29}$$

The second derivative represents the variance of $P(t)$ and, hence, a measure of the width of $P(t)$:

$$\tau^2 = \frac{\int_0^\infty (t - \delta)^2 P dt}{\int_0^\infty P dt} = \frac{\partial^2 \ell n p}{\partial s^2}\bigg|_{s=0}. \tag{30}$$

The third derivative

$$\eta^3 = \frac{\int_0^\infty (t-\delta)^3 P dt}{\int_0^\infty P dt} = \left.\frac{\partial^3 \ell n p}{\partial s^3}\right|_{s=0} \tag{31}$$

is generally called the "skewness" of the distribution $P(t)$. The ratio η/τ is a measure of the asymmetry of P and, as we shall see later, permits an immediate estimate of the value of $\gamma_\infty z$ without the knowledge of any other fiber parameters.

The fact that the Laplace term $ns/2c$ appears in (9) as part of the sum $A\sigma^2 = A + ns/2c$ permits us to use the relation

$$\left.\frac{\partial^m p(\theta, z, s)}{\partial s^m}\right|_{s=0} = \left(\frac{n}{2c}\right)^m \frac{\partial^m p(\theta, z, 0)}{\partial A^m}, \tag{32}$$

which will greatly simplify the following calculations.

Let us now apply (30) and (31) to the general solution (12) assuming again the special but practical condition $\Theta_o = \Theta_\infty$. We obtain

$$\delta_P(\theta) = \frac{T}{2}\left[\gamma_\infty z + \left(\frac{\theta^2}{\Theta_o^2} - \frac{1}{2}\right)(1 - e^{-2\gamma_\infty z})\right] \tag{33}$$

for the mean delay (in addition to the overall delay nz/c) and

$$\tau_P(\theta) = \frac{T}{2}\left[\gamma_\infty z + \left(\frac{\theta^2}{\Theta_o^2} - \frac{5}{4}\right) - 2\gamma_\infty z\left(2\frac{\theta^2}{\Theta_o^2} - 1\right)e^{-2\gamma_\infty z} + e^{-2\gamma_\infty z} - \left(\frac{\theta^2}{\Theta_o^2} - \frac{1}{4}\right)e^{-4\gamma_\infty z}\right]^{\frac{1}{2}} \tag{34}$$

for the half-width of the pulse. Figure 2 shows δ_P and τ_P plotted as a function of $\gamma_\infty z$ for $\theta = 0$ and $\theta = \Theta_o$. At first, a replica of the input pulse ($\tau = 0$) propagates in every mode without broadening and merely suffers a mode-dependent delay $n\theta_z^2/2c$, as we learned already from (18). Very soon, however, the pulses in the individual modes widen; they begin to overlap even before the length $1/\gamma_\infty$ is reached. Once $1/\gamma_\infty$ is passed, the pulse width in all modes increases mainly as $T(\gamma_\infty z)^{\frac{1}{2}}$. Compared to this increase, delay and pulse width differences in different modes become negligible since they cease to increase for large z. Specifically,

$$\delta_P(\theta) = \frac{T}{2}\left(\gamma_\infty z - \frac{1}{2} + \frac{\theta^2}{\Theta_o^2}\right), \qquad \text{for } \gamma_\infty z \gg 1 \tag{35}$$

and

$$\tau_P(\theta) = \frac{T}{2}\left(\gamma_\infty z - \frac{5}{4} + \frac{\theta^2}{\Theta_o^2}\right)^{\frac{1}{2}} \qquad \text{for } \gamma_\infty z \gg 1. \tag{36}$$

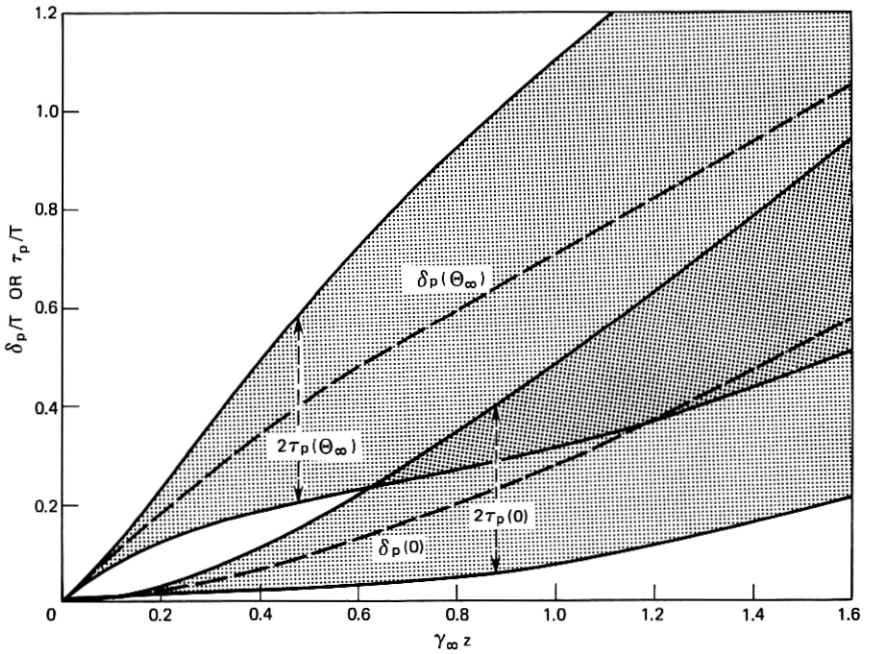

Fig. 2—Delay and time spread of the fiber output on axis and at an angle $\theta = \Theta_\infty$.

To calculate delay and width of the impulse response $Q(t)$, we must first apply the integration (19) to the general solution (12). This yields

$$q = \pi\Theta_0^2(\sigma \sinh \sigma\gamma_\infty z + \cosh \sigma\gamma_\infty z)^{-1}. \tag{37}$$

Now, by forming the first and second derivative of q according to (27) and (28), we obtain

$$\delta_Q = \frac{T}{2}\left[\gamma_\infty z + \frac{1}{2}(1 - e^{-2\gamma_\infty z})\right] \tag{38}$$

and

$$\tau_Q = \frac{T}{2}\left[\gamma_\infty z(1 - 2e^{-2\gamma_\infty z}) + \frac{3}{4} - e^{-2\gamma_\infty z} + \frac{1}{4}e^{-4\gamma_\infty z}\right]^{\frac{1}{2}}. \tag{39}$$

The ratio τ/T is shown in Fig. 3 plotted versus the normalized fiber length $\gamma_\infty z$. For $z \ll 1/\gamma_\infty$, the width τ approaches $T\gamma_\infty z$, as expected for negligible coupling. At $z = 1/4\gamma_\infty$, τ begins to follow a new asymptote

$$\tau = (T/2)(\gamma_\infty z)^{\frac{1}{2}}. \tag{40}$$

The quality of the approximation (40) is amazingly good even for small z.

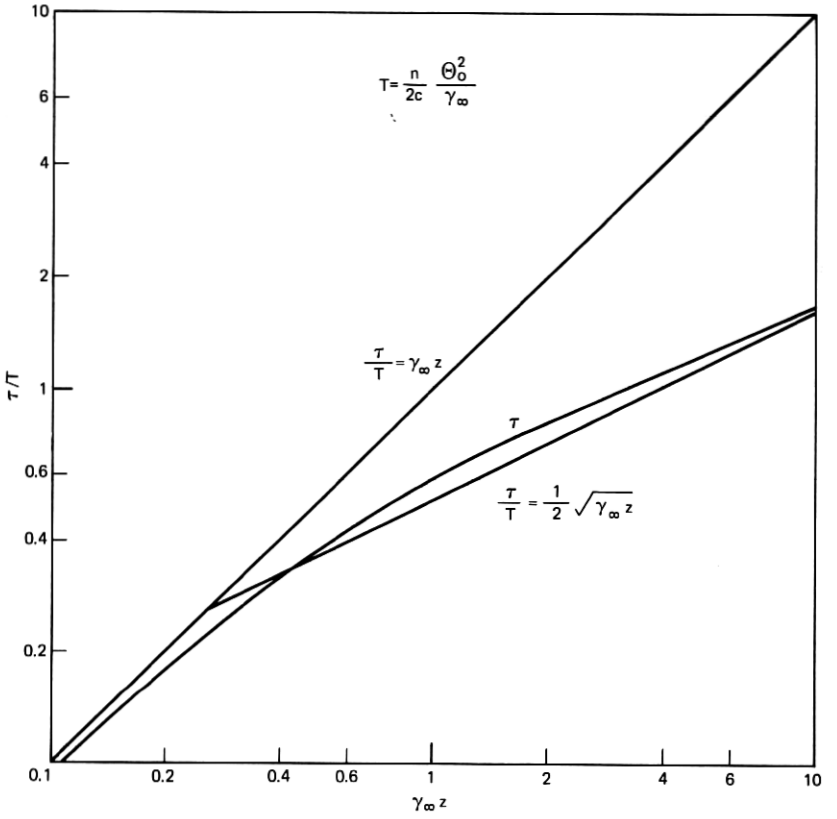

Fig. 3—Relative width of the impulse response plotted versus the normalized fiber length. The two straight lines show the asymptotic behavior for very short and very long fibers.

The amount by which τ deviates from $T\gamma_\infty z$ indicates the (desirable) effect of coupling: The width of the impulse response increases less with coupling than without,[6] the increase being proportional to $z^{\frac{1}{2}}$ rather than z.

V. SOME GENERAL RESULTS FOR LONG FIBERS

The simple approximation (40) can be obtained directly from (23) if σ in the denominator of that equation is set equal to unity. In this case,

$$q = \pi\Theta_\infty^2 \exp(-\sigma\gamma_\infty z) \tag{41}$$

independent of the input condition. By applying (32) to the approxi-

mation (41), we obtain

$$\frac{\int_0^\infty t^m Q dt}{\int_0^\infty Q dt} = -\left(\frac{n}{2c}\right)^m \frac{\partial^m}{\partial A^m}(-\gamma_\infty z) \tag{42}$$

where Q is the inverse Laplace transform of $q(s)$ and hence the impulse response as before. Equation (42) is an important and powerful relation which permits us to calculate all moments of the impulse response from the steady-state loss coefficient of the *time-independent* power flow equation.

If we let $m = 2$ in (42), we obtain (40) as expected. For $m = 3$ we have

$$\eta = \frac{T}{2}(3z\gamma_\infty)^{\frac{1}{3}} \tag{43}$$

which according to its definition (31) describes the "skewness" of $Q(t)$. The ratio

$$\eta/\tau = (9/\gamma_\infty z)^{1/6} \tag{44}$$

is a measure of the asymmetry of the impulse response. For large z, η/τ approaches zero and, hence, $Q(t)$ becomes a symmetric function. We can compute this function by introducing $t = t' + T\gamma_\infty z/2$ with $t' \ll T\gamma_\infty z/2$ in (24). The impulse response

$$Q(t) = \Theta_\infty^2 (2\pi/\gamma_\infty z)^{\frac{1}{2}} \exp(-\gamma_\infty z - 2t'^2/T^2\gamma_\infty z) \tag{45}$$

is then Gaussian in time with the variance τ of (40).

The asymmetry parameter (44) can be used to determine γ_∞. Particularly if merely the order of magnitude of γ_∞ is of interest, this can be obtained, with some experience, from a quick look at the asymmetry of the impulse response.

Another conveniently measurable fiber characteristic is the angular width Θ_∞ of the steady-state mode distribution. It can be obtained from a scan of the (angular) far-field distribution at the end of a long fiber ($z > 1/\gamma_\infty$). If we define the effective numerical aperture NA of the fiber as the sine of the apex angle of this cone of radiation (measured at the $1/e$-points of the intensity), then

$$\text{NA} = n \sin \Theta_\infty \approx n\Theta_\infty. \tag{46}$$

Using (15), (16), (25), and (40), we can now write the width of the impulse response as

$$\tau = \frac{(\text{NA})^2}{2nc}(z/4\gamma_\infty)^{\frac{1}{2}}. \tag{47}$$

This formula clearly shows the improvement, and the penalty, that results from coupling. Uncoupled, uniformly attenuated modes cause the impulse response to broaden to an effective width of $z(\mathrm{NA})^2/2nc$ in z km of fiber. This width can be reduced by a factor $(4\gamma_\infty z)^{\frac{1}{2}}$ in exchange for an increase in the overall attenuation by $4.35\gamma_\infty$ dB/km.

The physical contents of these results can best be summarized if we define a "coupling length" $L = 1/4\gamma_\infty$. As shown in Fig. 3, this length marks the point at which the width of the impulse response changes from a linear to a square-root dependence on length. Together with this change, the impulse response undergoes a transition from the exponential shape (21) to the Gaussian shape (45). The inverse of the coupling length (in km) is very nearly equal to the excess loss (in dB/km) incurred because of the coupling phenomenon.

Equation (47) as well as the previous results are limited to fibers in which the coupling coefficient D is independent of θ. The study of liquid-core fibers, on the other hand, has given us reason to believe that, in some fibers, D decreases with increasing θ. This characteristic could have a desirable effect on the impulse response and the excess loss, since it reduces the power flow toward the lossy modes (large angles) while, at the same time, enhancing the coupling among all other modes. We therefore studied the general case

$$D(\theta) = D_o \theta^{-\nu}, \qquad \nu = 0, 1, 2, \ldots, \tag{48}$$

in some detail.

The steady-state parameters Θ_∞ and γ_∞ can be obtained as general functions of A, D_o, and ν by using the Rayleigh-Ritz procedure.[9] Due to (42), twofold derivation of γ_∞ with respect to A then yields directly the effective width of the impulse response. This calculation leads to

$$\tau = \frac{(\mathrm{NA})^2}{2nc}\left[z/(4+\nu)\gamma_\infty\right]^{\frac{1}{2}} \tag{49}$$

where $\mathrm{NA} = n\Theta_\infty$ denotes the effective width of the output radiation as before. For $\nu = 0$, (49) reduces to (47). An exponent $\nu > 0$ indeed narrows the impulse response, although not very significantly. For $D = D_o/\Theta^4$, for example (a strong angular dependence indeed), τ is only 0.7 times narrower than in the case $D = \text{const}$.

Another limitation of these results is the requirement that $\Theta_\infty \ll (2\Delta)^{\frac{1}{2}}$. If this is not the case, the steady-state distribution is generally determined by a sharply rising loss term at $\theta_{\max} = (2\Delta)^{\frac{1}{2}}$ rather than by the quadratic term $A\theta^2$. Under these conditions we find that the functional relation (47) still holds, although with different

coefficients, so that for practical distributions $D(\theta)$ the width τ can be up to three times smaller than indicated by (47) or (36).

As a typical example, we shall use (36) to compute the data rates achievable. Let us assume that we had means to design and manufacture a coupling structure in the fiber which produced the desired excess loss γ_∞ and the desired numerical aperture. For simplicity we assume the input pulse to be somewhat narrower than the fiber impulse response so that (36) gives a good measure of the half-width of the expected output pulse. We then choose a data rate

$$B = 1/2\tau. \tag{50}$$

We assume the core loss common to all modes to be 4 dB/km and allow 50 dB of loss between repeaters.

Using (36) we can then calculate the excess loss and the repeater spacing necessary for a desired data rate. These results are plotted in Fig. 4. A 1-dB/km excess loss decreases the possible repeater spacing by only 25 percent but, at the same time, triples the data rate. An attempt to further increase the data rate by even more coupling is costly:

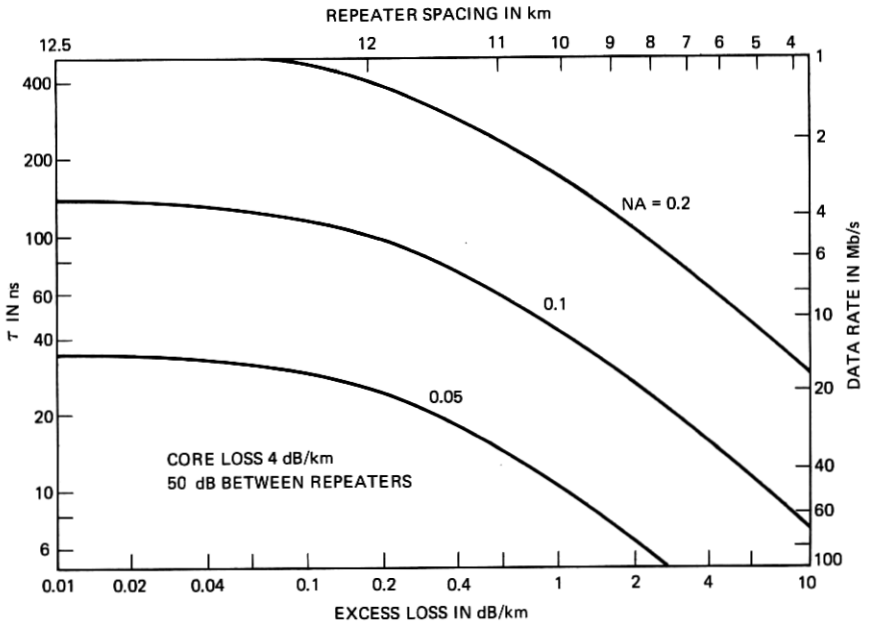

Fig. 4—Width of the impulse response plotted versus the excess loss incurred because of coupling for 4 dB/km core attenuation and 50 dB loss between repeaters. Right side shows equivalent data rates. Repeater spacing is shown at the top.

Another threefold increase in the data rate requires 4 dB/km excess loss, and divides the repeater spacing in half. The results of Fig. 4, of course, are based on a uniform coupling distribution and an excess loss increasing as θ^2. As mentioned earlier, more favorable distributions could result in an impulse response permitting a higher data rate, although there may be practical limitations to the extent of this improvement.

VI. CONCLUSIONS

The description of fiber modes by a continuum results in a partial differential equation whose solution yields the response function of the fiber. We find a characteristic length indicating the region in which the impulse response changes from an exponential to a Gaussian shape. Beyond this length, the width of the impulse response increases only as the square root of the fiber length. In practical fibers, the inverse of this length turns out to be proportional to the excess loss incurred because of the coupling phenomenon. The latter may represent a practical limit to the improvement that can be gained from coupling. As an example, we find a data rate of 12 Mb/s achievable for 10 km repeater spacing and an effective numerical aperture of 0.1. The data rate is inversely proportional to the square of the numerical aperture. Thus half the numerical aperture permits a fourfold increase of the data rate. Another increase of the data rate without a penalty in loss or numerical aperture is theoretically possible by artificially creating a more suitable coupling characteristic in the fiber, but it seems that the technological requirements for doubling or tripling the data rate in this way are high.

VII. ACKNOWLEDGMENTS

Stimulating discussions with Mrs. L. Wilson and Messrs. E. A. J. Marcatili, J. McKenna, and S. D. Personick are gratefully acknowledged.

REFERENCES

1. Dyott, R. B., and Stern, J. R., "Group Delay in Glass Fiber Waveguide," Elec. Lett., *7*, 1971, pp. 82–84.
2. Gloge, D., Chinnock, E. L., and Lee, T. P., "Self-Pulsing GaAs Laser for Fiber Dispersion Measurements," IEEE J. Quantum Elec., *QE-8*, 1972, pp. 844–846.
3. Gloge, D., Chinnock, E. L., Standley, R. D., and Holden, W. S., "Dispersion in a Low-Loss Multimode Fiber Measured at Three Wavelengths," Elec. Lett., *8*, 1972, pp. 527–529.
4. Gloge, D., Tynes, A. R., Duguay, M. A., and Hansen, J. W., "Picosecond Pulse Distortion in Optical Fibers," IEEE J. Quantum Elec., *QE-8*, 1972, pp. 217–221.

5. Gloge, D., "Optical Power Flow in Multimode Fibers," B.S.T.J., *51*, No. 8 (October 1972), pp. 1767–1783.
6. Personick, S. D., "Time Dispersion in Dielectric Waveguides," B.S.T.J., *50*, No. 3 (March 1971), pp. 843–859.
7. Marcuse, D., "Pulse Propagation in Multimode Dielectric Waveguides," B.S.T.J., *51*, No. 6 (July-August 1972), pp. 1199–1232.
8. Gloge, D., "Weakly Guiding Fibers," Appl. Opt., *10*, 1971, pp. 2252–2258.
9. Morse, P. M., and Feshbach, H., *Methods of Theoretical Physics*, vol. II, New York: McGraw-Hill, 1953, p. 1115.